Theory of multiferroic behavior in cycloidal helimagnets

2008 J. Phys.: Condens. Matter 20 434207

(http://iopscience.iop.org/0953-8984/20/43/434207)

J. Phys.: Condens. Matter **20** (2008) 434207 (7pp) doi:10.1088/0953-8984/20/43/434207

Theory of multiferroic behavior in cycloidal helimagnets

Naoto Nagaosa

Department of Applied Physics, University of Tokyo, 7-3-1, Hongo, Tokyo 113-8656, Japan
and
Cross-Correlated Materials Research Group (CRMG), RIKEN, 2-1, Horosawa, Wako,
Saitama 351-0198, Japan

Received 3 March 2008
Published 9 October 2008
Online at stacks.iop.org/JPhysCM/20/434207

Abstract

Theories of multiferroic behavior of cycloidal helimagnets are reviewed from the viewpoint of the spin current or vector spin chirality. Relativistic spin–orbit interaction leads to the coupling between the spin current and the electric polarization, and hence the ferroelectric and dielectric responses are a new and important probe for the spin states and their dynamical properties. Microscopic theories on the ground state polarization for various electronic configurations, the collective modes including the electromagnon, and the serious treatment of classical/quantum fluctuations are discussed with comparison to experimental results.

(Some figures in this article are in colour only in the electronic version)

1. Introduction and qualitative argument

Electromagnetism is established by Maxwell equations, which combine electricity and magnetism to reach the idea of a unified electromagnetic field. In other words, the electric and magnetic fields are the two sides of the single field A_μ (vector potential). This unifying principle has explained and predicted many new phenomena such as the electromagnetic wave. Another crucial point here is that electromagnetism is perfectly consistent with the principle of relativity. Due to the Lorentz transformation, the magnetic and electric fields are transmuted to each other in the moving frame. By this principle, for example, the moving magnetic moment can be coupled to the electric field. Thus, many of the electromagnetic phenomena are relativistic in nature, even though the large velocity of light c makes them rather small.

Let us turn to the electrons in solids, where the charge and spin degrees of freedom determine their electric and magnetic properties. Therefore, it is natural to ask the following question: *what is the electromagnetism in solids?* Of course, the electromagnetic responses of a solid are described by the response function $K_{\mu\nu}(q,\omega)$ ($\mu,\nu = 0,1,2,3$; q, momentum; ω, frequency), which connects the current J_μ to the external electromagnetic field A_ν as $J_\mu = K_{\mu\nu}A_\nu$. This response function combined with the Maxwell equations describes all the electromagnetic phenomena in the linear response regime. What we are interested in here is the microscopic mechanism to determine this $K_{\mu\nu}(q,\omega)$. To answer this question, we should start with the relativistic Dirac equation. However, in condensed matter physics, usually the non-relativistic Schrödinger equation is used to describe the electrons. This is because the velocity v of the electrons is assumed to be slow in solids compared with that of light c, which is in sharp contrast to high energy particles in cosmic rays for example. When one consider more carefully, however, the velocity of electrons is not so small compared with c, especially when it is bound near the nucleus with strong potential. This is described by the so-called spin–orbit interaction, whose Hamiltonian reads

$$H_{\mathrm{SO}} = \frac{e\hbar}{2m^2c^2}(\vec{p} \times \nabla V(r)) \cdot \vec{s} \tag{1}$$

where the notations are standard. For the centrosymmetric potential $V(r) = V(|r|)$, equation (1) is reduced to

$$H_{\mathrm{SO}} = \lambda \vec{\ell} \cdot \vec{s} \tag{2}$$

with $\vec{\ell}$ being the orbital angular momentum $\vec{\ell} = \vec{r} \times \vec{p}$. This λ is called the spin–orbit interaction constant, and is proportional to Z^2, with Z being the atomic number. The orbital of the electron is more and more localized near the nucleus as Z increases, and hence λ is also. Therefore, the spin–orbit interaction is stronger for heavier atoms, and compared with free electrons in vacuum the strength of the relativistic effect can be enhanced by a factor of $\sim 10^6$. In the 3d electrons in transition-metal oxides, which are the main focus in this article,

λ is typically of the order of 10–20 meV. It is smaller than the crystal field splitting, which is of the order of 0.5–1 eV, but still has novel consequences, as described below.

In the cubic crystal field, the fivefold degenerate d orbitals are split into threefold degenerate t_{2g} orbitals (xy, yz, zx orbitals) with lower energy, and doubly degenerate e_g orbitals ($x^2 - y^2$, $3z^2 - r^2$ orbitals) with higher energy. The orbital angular momentum has no matrix elements within the e_g orbitals, i.e. the orbital angular momentum is quenched in e_g orbitals, while it is finite within t_{2g} orbitals. However, it should be noted that $\vec{\ell}$ has matrix elements between the e_g and t_{2g} orbitals. Therefore, even when the t_{2g} orbitals are fully occupied, the spin–orbit interaction plays some role, as discussed below.

The magnetoelectric (ME) effect is induced by this very relativistic effect in solids, i.e. the spin–orbit interaction. The linear ME effect is symbolically written as [1, 2]

$$\begin{aligned} P &= \alpha H \\ M &= \alpha^{\mathrm{t}} E \end{aligned} \tag{3}$$

where α is the ME tensor and α^{t} is its transposed tensor. From the symmetry point of view, time-reversal symmetry T and space-inversion symmetry I are crucial. In order to have a finite α, both T and I must be broken, since P and M have the opposite symmetry for both T and I. The I-symmetry breaking in insulators is naturally accompanied by ferroelectricity, while the T-symmetry by magnetism. Therefore, the coexistence of both orders, i.e. the multiferroics, will lead to an enhanced ME effect.

One important clue to consider the coupling between the magnetism and electric polarization is the current of the spins, i.e. the spin current. Spin current is I-symmetry odd and T-symmetry even, because it is the product of the velocity and spin operators. This spin current has the same symmetry as the electric polarization, and hence it is natural to consider the coupling between the two. Actually, this is the case when one considers the duality in electromagnetism. In other words, a circulating magnetic field is induced by the charge current, while if the magnetic monopole existed in nature its motion would produce an electric field around it via the duality principle [3]. Of course there is no magnetic monopole, but the magnetic dipole exists, and its motion, i.e. the magnetic dipole current, produces an electric field, which is given by the superposition of the two shifted circulating electric fields and is perpendicular to the direction of the spin polarization and direction of the flow. The magnetic dipole moment is accompanied by the spin, and hence the spin current produces the electric field. More explicitly, the spin current is the tensor quantity J^i_j with the two indices corresponding to the direction of flow j and the direction of the spin polarization i. Therefore, the electric field or the electric polarization is perpendicular both to i and j, which is expressed by

$$P_k \propto \varepsilon_{kij} J^i_j \tag{4}$$

where ε_{kij} is the totally anti-symmetric tensor. Therefore, spin current produces electric polarization. Then, the next question is how to create spin current in magnetic systems.

To answer to this question, we need to look at the quantum nature of the spin, which is represented by the commutation relation of the spin components as

$$[S^\alpha, S^\beta] = \mathrm{i}\hbar\varepsilon_{\alpha\beta\gamma} S^\gamma. \tag{5}$$

This relation is translated into

$$[S^z, S^\pm] = \pm\mathrm{i}\hbar S^\pm, \tag{6}$$

where $S^\pm = S^x \pm \mathrm{i}S^y$. Let us define the 'phase' θ related to the xy-component of the spin as $S^\pm \sim \mathrm{e}^{\pm\mathrm{i}\theta}$. Then the commutation relation equation (5) can be translated to

$$[S^z, \theta] = \mathrm{i}\hbar. \tag{7}$$

This is analogous to the relation between the position x and momentum p in the quantum mechanics of a single particle, or that between the particle number n and the phase φ of the bosonic field operator. From the experience of the latter system, i.e. the Bose condensed state, which corresponds to the magnetically ordered state, the twist of the phase produces the super-flow of its canonical conjugate quantity. Applying this idea to equation (7), we conclude that the two non-collinear spins with different θ-values coupled by the exchange interaction lead to the super-spin current [4]. This super-spin current leads to the electric polarization $\vec{P}$ as given by

$$\vec{P} = \eta \vec{e}_{ij} \times (\vec{S}_i \times \vec{S}_j), \tag{8}$$

where η is a coupling constant proportional to the spin–orbit interaction. This scenario is embodied by the following cluster model of magnetic ions sandwiching an oxygen atom.

2. Cluster model

The magnetic exchange interaction between the localized spins is one of the most important topics in the physics of strongly correlated electronic systems. Anderson's idea for the super-exchange interaction is to consider the hybridization of the d orbital of the magnetic ions and the p orbitals of the oxygen atom. The Coulomb interaction on d orbitals leads to the magnetic moment formation. The total energy depends on the relative direction of these two spins through the oxygen atom, which is called the super-exchange interaction [5]. We have generalized this consideration to take into account the relativistic spin–orbit interaction, through which the directions of the spins affect the hybridization between p and d orbitals and lead to the electric polarization [4]. More explicitly, the model is schematically shown in figure 1.

We considered the simplest case, where the threefold degenerate t_{2g} orbitals under cubic crystal field are further split into Γ_8 and Γ_7 states by the spin–orbit interaction. Focusing on the doubly degenerate Γ_7 states, which we assumed to be singly occupied, we construct the effective Hamiltonian for the hybridized p and d orbitals, and their magnetic ordering, which we describe in terms of the mean field theory. In other words, we apply the Weiss field at each magnetic site in the directions of $\vec{e}_1$ and $\vec{e}_2$, respectively, which are non-collinear in general. In this approximation, the problem is reduced to that

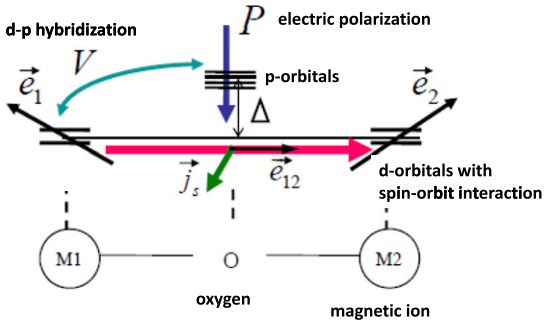

Figure 1. The cluster model for the electric polarization of magnetic origin. The magnetic ions with d orbitals sandwich an oxygen atom. The spin current represented by the thick arrow pointing to the right with the spin polarization perpendicular to it produces the electric polarization (arrows pointing downward).

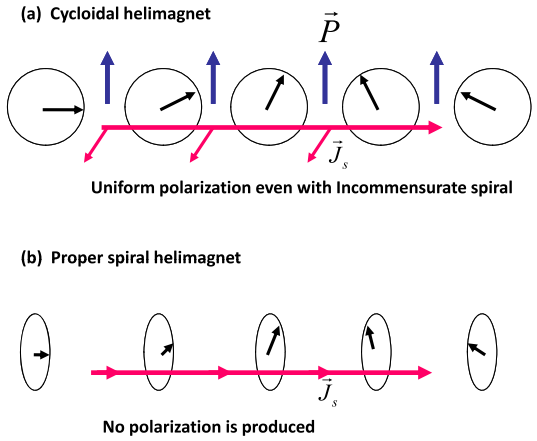

Figure 2. The cycloidal (a) and proper spiral (b) helimagnets. Due to the relation between the spin current $\vec{J}_s$ and the bond direction, only the cycloidal structure leads to ferroelectricity.

of a single particle, and the ground state can be obtained easily by diagonalizing a small Hamiltonian matrix.

The electric polarization comes from the matrix elements $I = \langle p_x|z|d_{zx}\rangle$ etc, and the total contribution is given by

$$\vec{P} \cong -\frac{4e}{9}\left(\frac{V}{\Delta}\right)^3 I\vec{e}_{12} \times (\vec{e}_1 \times \vec{e}_2). \tag{9}$$

where $\vec{e}_{12}$ is the unit vector connecting the two magnetic ions and $\Delta(V)$ is the energy difference (hybridization) between the p orbital and the d orbital. This expression is perfectly consistent with the above consideration in section 1, and the spin current is the key concept here. It is also confirmed in the case of double exchange interaction where the Γ_7 states are half-filled for each site.

This analysis leads to the prediction of multiferroic behavior of the various helimagnets. From equation (8) or (9), it is concluded that a helical magnetic structure with a spin spiral plane including the direction of the spiral wavevector results in a ferroelectric moment perpendicular to it. (figure 2(a)). This is distinct from the conventional improper ferroelectricity in the sense that even the incommensurate structure leads to *uniform* polarization. On the other hand, a proper spiral structure does not produce electric polarization (figure 2(b)). This strong directional dependence of the spin and polarization is an important consequence of spin current induced ferroelectricity. Before this theory was published, Kimura *et al* [6–8] discovered a novel ferroelectric state driven by the magnetic phase transition in $RMnO_3$. After the present theory was published, it was revealed that the magnetic structure is the cycloidal one and the above scenario has been established for this material [9–12]. Mostovoy [13] developed a phenomenological theory on the similar mechanism of multiferroic behavior. A theory taking into account the atomic displacement has also been proposed [14]. A systematic discussion of multiferroic behaviors based on group theory has been also developed [15]. Many other multiferroic materials have been studied experimentally, and the spin current mechanism of the multiferroic behaviour has been confirmed [16–19].

The above analysis has been done for a specialized model, and one might be suspicious about its validity in the general case. To study all the possible microscopic mechanisms of the electric polarization of magnetic origin, we have extended the above analysis to the generic electronic configurations [20, 21]. This is also urgent from the viewpoint of the experiments, since we now have a variety of multiferroic materials such as $RMnO_3$ [6–12], $Ni_3V_2O_8$ [22], $Ba_{0.5}Sr_{1.5}Zn_2Fe_{12}O_{22}$ [23], $CoCr_2O_4$ [24], $MnWO_4$ [25], $CuFeO_2$ [26], $LiCuVO_4$ [27], and $LiCu_2O_2$ [28].

Here we take the perturbative approach in both V/Δ and λ/Δ, where V and Δ represent the hybridization and the charge transfer energy between the transition-metal (TM) d and ligand (L) p orbitals, and λ is the spin–orbit interaction energy [20, 21]. Note that the spin–orbit interaction has the matrix elements within the t_{2g} orbitals and between the t_{2g} and e_g orbitals, while not within the e_g orbitals. The spin–orbit interaction at the ligand oxygen site is also considered. In the previous treatment, we have considered only the doubly degenerate Γ_7 states after the splitting by the spin–orbit interaction λ, and hence the expression for the electric polarization did not include λ. In the present approach, on the other hand, it is proportional to λ since we take the first-order perturbation, which is more realistic because $\lambda \sim 20$ meV is smaller than the energy denominators such as Δ, of the order of a fraction of an eV at least.

Based on this analysis, the polarization $\pm P_{r+\frac{e}{2}}$ on the bond between the sites $\boldsymbol{r}$ and $\boldsymbol{r}+\boldsymbol{e}$ is summarized as

$$\begin{aligned}\boldsymbol{P}_{r+\frac{e}{2}} = {} & P^{\mathrm{ms}}(\boldsymbol{m}_r \cdot \boldsymbol{m}_{r+e})\boldsymbol{e} + P^{\mathrm{sp}}\boldsymbol{e} \times (\boldsymbol{m}_r \times \boldsymbol{m}_{r+e}) \\ & + P^{\mathrm{orb}}\left[(\boldsymbol{e}\cdot\boldsymbol{m}_r)\boldsymbol{m}_r - (\boldsymbol{e}\cdot\boldsymbol{m}_{r+e})\boldsymbol{m}_{r+e}\right],\end{aligned} \tag{10}$$

where $\boldsymbol{m}_r$ is the spin direction at $\boldsymbol{r}$. $P^{\mathrm{ms}} \propto (V/\Delta)^3$ is the polarization due to the magnetostriction, which does not require the spin–orbit interaction, $P^{\mathrm{sp}} \propto (\lambda/\Delta)(V/\Delta)^3$ is that due to the spin current as discussed above, and $P^{\mathrm{orb}} \sim \min(\lambda/V, 1)(V/\Delta)$ is the term which is nonzero for the partially filled t_{2g} orbitals found in [20]. These three contributions appear differently depending on the wavevector of the polarization as summarized in table 1. Therefore, the experiments with momentum resolution such as x-ray and neutron scattering can contribute to the identification of the microscopic mechanism of the electric polarization.

Table 1. Fourier components of the electric polarization, which must be associated with the lattice modulation.

Fourier component	Mechanism	
$\boldsymbol{P}(\mathbf{o})$	$P^{\rm sp}$	$-\boldsymbol{e}\times(\boldsymbol{m}_1\times\boldsymbol{m}_2)\sin\boldsymbol{Q}\cdot\boldsymbol{e}$
$\boldsymbol{P}(\pm(\pi\boldsymbol{e}+\boldsymbol{Q}))$	$P^{\rm ms}$	$\boldsymbol{e}[\boldsymbol{m}_0\cdot(\boldsymbol{m}_1\pm{\rm i}\boldsymbol{m}_2)]\cos[\boldsymbol{Q}\cdot\boldsymbol{e}/2]$
$\boldsymbol{P}(\pm(\pi\boldsymbol{e}+2\boldsymbol{Q}))$	$P^{\rm ms}$	$\boldsymbol{e}(\boldsymbol{m}_1^2+\boldsymbol{m}_2^2)/4$
$\boldsymbol{P}(\pm\boldsymbol{Q})$	$P^{\rm orb}$	$\mp{\rm i}[(\boldsymbol{e}\cdot\boldsymbol{m}_0)\boldsymbol{m}_\pm+(\boldsymbol{e}\cdot\boldsymbol{m}_\pm)\boldsymbol{m}_0]$
	$P^{\rm sp}$	$\mp\frac{1}{2}\boldsymbol{e}\times(\boldsymbol{m}_0\times\boldsymbol{m}_\mp)\sin[\boldsymbol{Q}\cdot\boldsymbol{e}/2]$
$\boldsymbol{P}(\pm2\boldsymbol{Q})$	$P^{\rm orb}$	$\mp\frac{1}{2}[(\boldsymbol{e}\cdot\boldsymbol{m}_\pm)\boldsymbol{m}_\pm]\sin\boldsymbol{Q}\cdot\boldsymbol{e}$

The electric polarization of magnetic origin in $TbMnO_3$ has been analyzed as follows. The electronic configuration of Mn^{3+} is $3d^4$. In other words, three electrons occupy the t_{2g} orbitals and one electron occupies one of the e_g orbitals, with all the spins parallel at each atom due to the Hund's coupling. Therefore, the dominant spin–orbit interaction channels are the t_{2g}–e_g mixing [29] and that on the oxygen p orbitals. We take the TM–O bond length 1.9 Å and the Clementi–Raimondi effective charges [30] $Z^{\rm eff}_{\rm Mn3d}=10.53$ and $Z^{\rm eff}_{\rm O2p}=4.45$. Other parameters are chosen as $V_l=2V_r=-V_{{\rm pd}\sigma}=-1.2$ eV, $U=3$ eV, and $E_{e_g}-E_{\rm p}=2$ eV. The spin–orbit couplings for the oxygen 2p and TM 3d orbitals are chosen as $\lambda_{\rm p}=25$ meV and $\lambda_{\rm d}=48$ meV [31]. With these values the uniform polarization along the c axis is estimated as $P^{\rm sp}_{\rm p}\sim 130\ \mu{\rm C\,m^{-2}}$ from the oxygen spin–orbit interaction, and $P^{\rm sp}_{t_{2g}\text{–}e_g}\sim 860\ \mu{\rm C\,m^{-2}}$ from the t_{2g}–e_g mixing with $\Delta_{\rm cf}=2$ eV and $E_{\rm JT}=1$ eV. The net value $P^{\rm sp}\sim 990\ \mu{\rm C\,m^{-2}}$ multiplied by $|\boldsymbol{m}_r\times\boldsymbol{m}_{r+e}|\approx\sin(0.28\pi)$ in equation (10) gives the uniform c-axis polarization of $\sim$760 $\mu{\rm C\,m^{-2}}$, in reasonable agreement with the experimental value in $TbMnO_3$ [8] ($\sim$700 $\mu{\rm C\,m^{-2}}$ at 10 K).

3. Collective modes of the cycloidal helimagnets

Up to now we have discussed the ground state properties of the multiferroic materials, focusing on the interplay between the magnetic and electric degrees of freedom. The next issue is the dynamical properties, which can be studied by infrared optical spectra and inelastic neutron scattering, Theoretically, the analysis of the collective modes in the cycloidal helimagnets is the first thing to do, which we describe in this section. Before going into detailed analysis, let us discuss the qualitative features of the spin waves in helimagnets. From the symmetry viewpoint, the order parameter of the usual collinear magnets such as ferromagnets and antiferromagnets is characterized by the group $SO(3)/U(1)$, since the rotation around the direction of the ordered moment remains intact. On the other hand, the helimagnetic order completely destroys the spin rotation symmetry and the order parameter belongs to $SU(2)$. Therefore, there are two Goldstone collectives modes in the case of collinear magnets, while there are three in helimagnets. These three collective modes correspond to the rotation of the ordered moments around three axes. When the rotation axis is perpendicular to the spin plane, it corresponds to the phase mode, while the other two correspond to the fluctuations of the spiral plane. The new aspect here is that the electric polarization is coupled to the magnetic moments as described in equation (8). It is easily seen that the polarization changes only when the spiral plane rotates around the direction of the wavevector, and the direction of the fluctuating polarization accompanies it. Therefore, the in-phase fluctuation of both the spiral plane and polarization forms a collective mode, called the electromagnon [32], a more detailed treatment of which is given below [33].

The spin wave theory of helimagnets was developed long ago by Nagamiya *et al* [34]. The key observation is the introduction of the rotating frame with the ordered moment. In this rotated frame, the ordered moments align ferromagnetically, and the complications related to the incommensurate structure can be avoided. We start with the following Hamiltonian for the spin $\vec{S}_n$ [33]:

$$H=H_1+H_2+H_3+H_4, \tag{11}$$

$$H_1=-\sum_{m,n}J(R_m-R_n)\vec{S}_m\cdot\vec{S}_n, \tag{12}$$

$$H_2=-\lambda\sum_m(\vec{u}_m\times\vec{e}_z)\cdot(\vec{S}_m\times\vec{S}_{m+1}), \tag{13}$$

$$H_3=\sum_m\left(\frac{\kappa}{2}\vec{u}_m^2+\frac{1}{2M}\vec{P}_m^2\right), \tag{14}$$

$$H_4=\sum_m D(S_m^y)^2, \tag{15}$$

where the displacement $\vec{u}$ represents the electric polarization, while the spin–lattice interaction λ stems from the relativistic spin–orbit interaction. Once the static displacement $\langle\vec{u}_j\rangle$ is nonzero and breaks the inversion symmetry, this turns into the DM interaction. In H_3, κ and M are the spring constant and the effective mass of $\vec{u}_m$, respectively. The term with the coefficient D in H_4 represents the easy plane spin anisotropy, and we assume that the ground state spin configuration on the plane perpendicular to the helical wavevector is ferromagnetic. Hence we shall focus on the wavenumber $q=q_z$ along the helical wavevector.

We consider the ground state spin configuration as $S_n^z=S\cos(QR_n+\phi)$, $S_n^x=S\sin(QR_n+\phi)$, $S_n^y=0$, and we derive the equations of motion for spins and displacements up to the linear order in the fluctuations of these quantities. In other words, this is the standard random-phase approximation (RPA), and the collective modes can be analyzed in this way. The nontrivial point here is to introduce a rotating local coordinate system ξ,η,ζ such that the ζ-axis coincides with the equilibrium spin direction at each site, the ξ-axis is perpendicular to this direction in the zx-plane, and the η-axis is parallel to the y-axis [34].

From the equations of motion, and the commutation relation, we can obtain the retarded Green function as $G^{\rm R}(AB;t-t')\equiv-{\rm i}\theta(t-t')\langle[A(t),B(t')]\rangle$, and its Fourier transform $G^{\rm R}(AB;\omega)\equiv\frac{1}{2\pi}\int_{-\infty}^{\infty}G^{\rm R}_{AB}(t){\rm e}^{{\rm i}\omega t}$ ($A,B=u_q,p_q,S_q^\xi,S_q^\eta$). The imaginary part of the ac susceptibility is also defined, as $\chi''(AB;\omega)\equiv-{\rm Im}\,G^{\rm R}(AB;\omega)$.

The effect of the coupling between the spins and polarization is usually very weak and difficult to observe in experiments such as neutron scattering experiments and antiferromagnetic resonance. Therefore, we will focus below

on the dynamical dielectric response, where the electromagnon can manifest itself in experiment. The dynamical dielectric function $\varepsilon_{yy}(\omega) = 1 - 4\pi(e^*)^2 G^{\mathrm{R}}(u_0 u_0; \omega)$, where e^* is the Born charge corresponding to the displacement u^y and

$$G^{\mathrm{R}}(u_0 u_0; \omega) = \frac{\omega^2 - \omega_p^2}{2\pi M(\omega^4 - (\omega_0^2 + \omega_p^2)\omega^2 + A(Q)D\omega_0^2)}, \tag{16}$$

where $\omega_p = \sqrt{A(Q)B(Q)}$ is the frequency of the spin plane rotation mode along the x-axis and $\omega_0 = \sqrt{\kappa/M}$ is that for the original phonon. Here $A(q) = 2S[J(Q) - \frac{J(Q+q)+J(Q-q)}{2} + \frac{2\lambda^2 S^2}{\kappa}\sin^2(qa/2)\sin^2(Qa)]$, $B(q) = 2S[J(Q) - J(q) + \frac{\lambda^2 S^2}{\kappa}\sin^2(Qa) + D]$. This response function has poles at $\omega_\pm$, which are explicitly given by

$$\omega_\pm^2 = \tfrac{1}{2}\left(\omega_0^2 + \omega_p^2 \pm \sqrt{(\omega_0^2 + \omega_p^2)^2 - 4A(Q)D\omega_0^2}\right). \tag{17}$$

Assuming $D, \lambda \ll \omega_0^2$, one can estimate $\omega_- \cong \sqrt{A(Q)D} \sim \sqrt{8SJD}$ and $\omega_+ \cong \omega_0$. With these frequencies, $\varepsilon_{yy}(\omega) = 1 + \sum_\pm \omega_\pm I_\pm/(\omega^2 - \omega_\pm^2)$ with the 'oscillator strengths' $I_\pm$ being given by $I_- = \frac{2(e^*)^2(\omega_p^2 - \omega_-^2)}{M\omega_-(\omega_+^2 - \omega_-^2)}$ and $I_+ = \frac{2(e^*)^2(\omega_+^2 - \omega_p^2)}{M\omega_+(\omega_+^2 - \omega_-^2)}$. Note that the oscillator strength, i.e. the integral $-\int_0^\infty \mathrm{d}\omega\, \varepsilon_{yy}(\omega)$, is given by $(\pi/2)(I_- + I_+)$. Since the '+'-mode is basically the original phonon mode, we consider only the new optical active mode, i.e. the '−'-mode, corresponding to the electromagnon [32, 33]. The low-frequency behavior of $\varepsilon_{yy}(\omega)$ is dominated by this electromagnon, having the oscillator strength $I_- \sim p^2\sqrt{J/D}$ as $D \to 0$. This means that the oscillator strength can be rather large when the anisotropy is small even though the spin–lattice coupling λ is small.

Interpretation of the experiments on the infrared absorption of $RMnO_3$ in the terahertz region [35] in terms of this electromagnon has been done in [33]. Assuming the exchange coupling J_1 between the nearest-neighbor spins as $8SJ_1 \cong 9$ meV for $PrMnO_3$ and $8SJ_1 \cong 2.4$ meV for $TbMnO_3$, $D \cong 0.4$ meV estimated from the neutron scattering experiment [36], and the spin–lattice coupling $\lambda \sim 1$ meV Å^{-1} [14], we can obtain the static displacement $u_m = 10^{-3}$ Å. The Born charge e^* can be estimated from the value of electric polarization with the above u_m. From the experimentally observed electric polarization along the c-axis $P_c \sim 0.2\ \mu$C cm^{-2} for $DyMnO_3$ [8], the Born charge e^* is $16e$, which is much greater than the unit charge. From these values, ω_- and I_- are independently estimated as $\omega_- \sim 10$ cm^{-1} and $I_- \sim 4$ cm^{-1}.

Pimenov *et al* [35] observed the peak of $\mathrm{Im}\,\varepsilon$ at around 20 cm^{-1}, with the magnitude of 1–2 in $GdMnO_3$ and $TbMnO_3$. This 20 cm^{-1} is identified with ω_-, and the integration of $-\mathrm{Im}\varepsilon_{yy}(\omega)$ over ω gives $I_- \sim 12$ cm^{-1}, which is a bit larger than the above theoretical estimate. Also, a neutron scattering experiment [37] reported the identification of one of the spin mode branches as the electromagnon.

However, recent experiments have revealed that the oscillator strength grows and this discrepancy increases even more as the temperature is further lowered [38, 39]. An even more serious puzzle is that the anisotropy of the optical absorption does not change even when the spiral plane changes from the bc- to the ac-plane, while the electric polarization associated with the electromagnon should change the direction. Therefore, the main contribution to the absorption in the terahertz region has been attributed to the two-magnon processes in [38], but this issue still remains an important topic to be studied.

4. Spin fluctuation and chiral spin liquid

As discussed above, the spin current or the vector spin chirality $\vec{S}_i \times \vec{S}_j$ is the key quantity to control the electric polarization. The ordered ground state and small fluctuation around it have been discussed up to now, but the spin fluctuation is sometimes rather large and a non-perturbative treatment is needed, as in the case of (quasi-) low-dimensional systems [40]. In particular, there have appeared quasi-one-dimensional [28, 41], and quasi-two-dimensional [22] helimagnetic systems.

There are many references discussing theoretically the possible chiral spin liquid state [42–49]. However, it usually appears only in a tiny region of the global phase diagram, and the physical mechanism for its appearance has not been understood yet. We have developed the phenomenological theory based on the Ginzburg–Landau free energy functional, to reveal the condition for the chiral spin liquid above the helimagnetic ordering. The spin in the helical Heisenberg magnets can be expressed in terms of two independent slowly varying fields as

$$\vec{S}_r \approx \vec{a}_r \cos \boldsymbol{Q}\cdot\boldsymbol{r} - \vec{b}_r \sin \boldsymbol{Q}\cdot\boldsymbol{r}, \tag{18}$$

while the GL-functional is given by [50]

$$\mathcal{H} \approx \int \mathrm{d}^d\boldsymbol{r}\Big[\frac{\mu}{2}(\vec{a}^2 + \vec{b}^2) + \frac{1}{2}\left((\nabla\vec{a})^2 + (\nabla\vec{b})^2\right) + \frac{u}{4}(\vec{a}^2 + \vec{b}^2)^2 + v((\vec{a}^2\vec{b}^2) - (\vec{a}\cdot\vec{b})^2)\Big] \tag{19}$$

with a_0 being the lattice constant. Quartic interaction terms with the coupling constants u and v can be obtained by softening the constraint that amplitudes of spins must be fixed, $\vec{S}(\boldsymbol{r})^2 \approx S^2$, and the original quartic term $\frac{u_0}{6}\int \mathrm{d}\boldsymbol{r}(\vec{S}_{\boldsymbol{r}}^2)^2$ results in $u = u_0 > 0$ and $v = v_0 = -u_0/3$. The deviation of the ratio v/u from $-1/3$ occurs due to the additional interactions and is an important parameter, as will be discussed below. The helical and collinear magnetic orders are described by $\langle\vec{a}\rangle \times \langle\vec{b}\rangle \neq \vec{0}$ and $\langle\vec{a}\rangle \times \langle\vec{b}\rangle = \vec{0}$, respectively. The vector-chiral order is characterized by $\langle\vec{a} \times \vec{b}\rangle \neq \vec{0}$.

The mean field phase diagram of the GL theory in equation (19) is a simple one. For a fixed $u > 0$, we can draw the phase diagram in the plane of μ (corresponding to the temperature) and v. For $v < 0$, the helimagnetic state is preferred, while the collinear state is favored by $v > 0$. Therefore, the phase diagram is that as shown schematically by the straight phase boundary lines in figure 3. The collinear and helimagnetic states are separated by the first-order phase transition. Then our aim is to study the effects of the (classical) fluctuation on this phase diagram. For that purpose, we employ the mode coupling approximation. The readers are referred to the original paper [40], and we discuss here the physical picture obtained by the analysis.

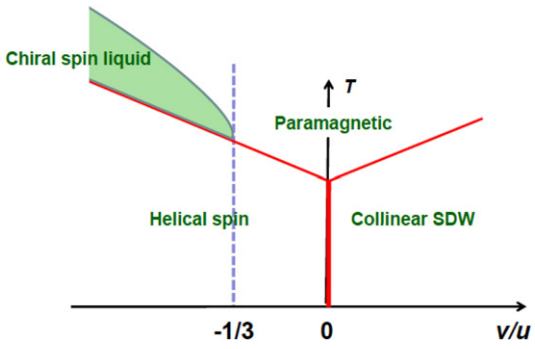

Figure 3. The phase diagram of the helimagnet described by equation (19) taking into account the spin fluctuation. The chiral spin liquid state is realized above the magnetic ordering for $v/u < -1/3$.

The mode coupling analysis enables a new composite order parameter such as $\langle \vec{a} \cdot \vec{b} \rangle$ and $\langle \vec{a} \times \vec{b} \rangle$ even without the magnetic ordering, i.e., $\langle \vec{a} \rangle = \langle \vec{b} \rangle = \vec{0}$. Considering that the canonical model for the helimagnet has the parameter $u = u_0 > 0$ and $v = v_0 = -u_0/3$, we will consider the possibility of nonzero $\langle \vec{a} \times \vec{b} \rangle$ below. Even though we are treating the classical field, the analogy to the electronic or bosonic system is useful here. In other words, the $\vec{a}$ and $\vec{b}$ fields correspond to the 'particle' fields while $\vec{a} \times \vec{b}$ to the pairing field. In this respect, it is crucial if the interaction between the $\vec{a}$ and $\vec{b}$ particles is repulsive or attractive. It turned out that the $\vec{a}$ and $\vec{b}$ fields are 'non-interacting' when $v/u = -1/3$, and $v/u < -1/3$ corresponds to the attractive interaction. Very similar to the BCS pairing instability, the pairing susceptibility of $\vec{a}$ and $\vec{b}$ fields diverges before the magnetic ordering occurs. This means that the chiral spin liquid state appears slightly above the helimagnetic ordering temperature as shown in figure 3. In this state, $\langle \vec{a} \times \vec{b} \rangle$ is finite while $\langle \vec{a} \rangle = \langle \vec{b} \rangle = \vec{0}$.

Now the physical mechanism for the deviation of v/u from $-1/3$ is discussed. There are several possible interactions giving the positive and negative contributions to this ratio. (i) The magnetostrictive interaction between the spins and phonons leads to a positive shift after integrating over the phonon degrees of freedom. (ii) The anti-symmetric DM coupling [51] between the nearest-neighbor spin pair $\vec{S}_r$ and the phonon contributes negatively to the ratio after integrating over the phonons. (iii) The four-spin ring-exchange interaction can contribute both positively and negatively [52, 53]. In other words, the kinetic ring-exchange process contributes positively while that of direct Coulomb interaction contributes negatively. When the negative contributions dominate over the positive ones, the chiral spin liquid state is expected to be observed above the magnetic ordering.

Recently, an experiment on $Gd(hfac)_3NITEt$ has appeared which found the two-step phase transition and suggested the chiral spin liquid state [41]. This is the quasi-one-dimensional system and Gd has spin 7/2. Therefore, it can be regarded as a strongly fluctuating classical helimagnet, and offers an ideal arena to test our theory described above.

The quantum mechanical fluctuation in a helimagnet is an interesting problem to be studied. As mentioned above, there have been many theoretical proposals for the ground state of a quantum helimagnet [47–49], but the finite temperature properties have not yet been studied. Recently, Furukawa *et al* [54] and Katsura *et al* [55] studied this problem in terms of the numerical method and Schwinger boson theory, respectively. The natures of the classical and quantum fluctuations are different and the phase diagram is quite different. The readers are referred to the references.

5. Summary and conclusions

In this article, we have reviewed the theoretical studies on multiferroic helimagnets from the viewpoint of the spin current or the vector spin chirality. The frustrated spin system is now viewed from the new aspects, i.e. the ferroelectric and dielectric response associated with the vector spin chirality. The ground and excited states are characterized by novel dielectric properties; i.e., the charge degrees of freedom in Mott insulators is not silent at all, and rich physics is found there.

From the viewpoint of spintronics, it is highly desirable to develop spintronics without dissipation. The magnetoelectric effect in insulators is a promising direction for this purpose, and we have shown above that the dissipationless spin current plays a crucial role there.

Acknowledgments

The author thanks H Katsura, A V Balatsky, S Onoda, H J Han, and C Jia for collaborations on the works reported here, and Y Tokura, T Arima, N Kida, M Sato, M Mosztovoy, D I Khomskii, and A Aharony and A Loidl for useful discussions. This work is supported by Priority Area Grants, Grants-in-Aid under grant Nos 15104006, 16076205, and 17105002, and NAREGI Nanoscience Project from the Ministry of Education, Culture, Sports, Science, and Technology, Japan.

References

[1] Curie P 1894 *J. Phys.* **3** 393
[2] Fiebig M 2005 *J. Phys. D: Appl. Phys.* **38** R123
[3] Aharonov Y and Casher A 1984 *Phys. Rev. Lett.* **53** 319
[4] Katsura H, Nagaosa N and Balatsky A V 2005 *Phys. Rev. Lett.* **95** 057205
[5] Anderson P W 1963 *Solid State Physics* vol 14, ed F Seitz and D Turnbull (New York: Academic) p 99
[6] Kimura T *et al* 2003 *Nature* **426** 55
[7] Kimura T *et al* 2003 *Phys. Rev.* B **68** 060403(R)
[8] Goto T *et al* 2004 *Phys. Rev. Lett.* **92** 257201
[9] Kenzelmann M *et al* 2005 *Phys. Rev. Lett.* **95** 087206
[10] Arima T, Tokunaga A, Goto T, Kimura H, Noda Y and Tokura Y 2006 *Phys. Rev. Lett.* **96** 097202
[11] Yamasaki Y *et al* 2007 *Phys. Rev. Lett.* **98** 147204
[12] Tokura Y 2006 *Science* **312** 1481
[13] Mostovoy M 2001 *Phys. Rev. Lett.* **96** 067601
[14] Sergienko I A and Dagotto E 2006 *Phys. Rev.* B **73** 094434
[15] Harris A B, Yildirim T, Aharony A and Entin-Wohlman O 2006 *Phys. Rev.* B **73** 184433
[16] Hur N *et al* 2004 *Nature* **429** 392

[17] Chapon L C *et al* 2004 *Phys. Rev. Lett.* **93** 177402
[18] Blake G R *et al* 2005 *Phys. Rev.* B **71** 214402
[19] Kimura T, Lawes G and Ramirez A P 2005 *Phys. Rev. Lett.* **94** 137201
[20] Jia C, Onoda S, Nagaosa N and Han J H 2006 *Phys. Rev.* B **74** 224444
[21] Jia C, Onoda S, Nagaosa N and Han J H 2007 *Phys. Rev.* B **76** 144424 (*Preprint* cond-mat/0701614)
[22] Lawes G, Harris A B, Kimura T, Rogado N, Cava R J, Aharony A, Entin-Wohlman O, Yildirim T, Kenzelmann M, Broholm C and Ramirez A P 2005 *Phys. Rev. Lett.* **95** 087205
[23] Kimura T, Lawes G and Ramirez A P 2005 *Phys. Rev. Lett.* **94** 137201
[24] Yamasaki Y, Miyasaka S, Kaneko Y, He J-P, Arima T and Tokura Y 2006 *Phys. Rev. Lett.* **96** 207204
[25] Taniguchi K, Abe N, Takenobu T, Iwasa Y and Arima T 2006 *Phys. Rev. Lett.* **97** 097203
[26] Kimura T, Lashley J C and Ramirez A P 2006 *Phys. Rev.* B **73** 220401
[27] Naito Y, Sato K, Yasui Y, Kobayashi Y, Kobayashi Y and Sato M 2006 *Preprint* cond-mat/0611659
[28] Park S, Choi Y J, Zhang C L and Cheong S-W 2007 *Phys. Rev. Lett.* **98** 057601
[29] Hu C D 2008 *Phys. Rev. Lett.* **100** 077202 (*Preprint* cond-mat/0608470)
[30] Clementi E and Raimondi D L 1963 *J. Chem. Phys.* **38** 2686
Clementi E, Raimondi D L and Reinhardt W P 1967 *J. Chem. Phys.* **47** 1300
[31] Kotochigova S, Levine Z H, Shirley E L, Stiles M D and Clark C W 1997 *Phys. Rev.* A **55** 191
Kotochigova S, Levine Z H, Shirley E L, Stiles M D and Clark C W 1997 *Phys. Rev.* A **56** 5191
[32] Chupis I E 2007 *Low Temp. Phys.* **33** 952 (*Preprint* cond-mat/0702636)
[33] Katsura H, Balatsky A V and Nagaosa N 2007 *Phys. Rev. Lett.* **98** 027203
[34] Nagamiya T 1967 *Solid State Physics* vol 20, ed F Seita, D Turnbull and H Ehrenreich (New York: Academic)
[35] Pimenov A *et al* 2006 *Nat. Phys.* **2** 97
[36] Kajimoto R *et al* 2005 *J. Phys. Soc. Japan* **74** 2430
[37] Senff D *et al* 2007 *Phys. Rev. Lett.* **98** 137206
[38] Kida N, Ikebe Y, Takahashi Y, He J P, Kaneko Y, Yamasaki Y, Shimano R, Arima T, Nagaosa N and Tokura Y 2007 *Preprint* 0711.2733
[39] Pimenov A *et al* 2008 *Phys. Rev.* B **77** 014438 (*Preprint* 0707.3614)
[40] Onoda S and Nagaosa N 2007 *Phys. Rev. Lett.* **99** 027206
[41] Cinti F *et al* 2008 *Phys. Rev. Lett.* **100** 057203
[42] Villain J 1977 *J. Phys. C: Solid State Phys.* **10** 4793
[43] Teitel S and Jayaprakash C 1983 *Phys. Rev.* B **27** 598
[44] Andreev A F and Grishchuk I A 1984 *Sov. Phys.—JETP* **60** 267
[45] Miyashita S and Shiba H 1984 *J. Phys. Soc. Japan* **53** 1145
[46] Lee S and Lee K-C 1998 *Phys. Rev.* B **57** 8472
[47] Hikihara T *et al* 2000 *J. Phys. Soc. Japan* **69** 259
[48] Chandra P, Coleman P and Larkin A I 1990 *J. Phys.: Condens. Matter* **2** 7933
[49] Balatsky A V and Abrahams E 1995 *Phys. Rev. Lett.* **74** 1004
[50] Kawamura H 1998 *J. Phys.: Condens. Matter* **10** 4707 and references therein
[51] Dzyaloshinskii I E 1957 *Sov. Phys.—JETP* **5** 1259
Moriya T 1960 *Phys. Rev.* **120** 91
[52] Schmidt H J and Kuramoto Y 1990 *Physica* C **167** 263
[53] Brehmer S *et al* 1999 *Phys. Rev.* B **60** 329
[54] Furukawa S, Sato M, Saiga Y and Onoda S 2008 *Preprint* 0802.3256
[55] Katsura H, Onoda S, Han J H and Nagaosa N 2008 *Preprint* 0804.0669